MHD orthogonal stagnation-point flow of a micropolar fluid with the magnetic field parallel to the velocity at infinity

Alessandra Borrelli

Dipartimento di Matematica e Informatica, Università di Ferrara, via Machiavelli 35, 44121 Ferrara Italy

Giulia Giantesio

Dipartimento di Matematica e Informatica, Università di Ferrara, via Machiavelli 35, 44121 Ferrara Italy

Maria Cristina Patria

Dipartimento di Matematica e Informatica, Università di Ferrara, via Machiavelli 35, 44121 Ferrara Italy

Abstract

An exact solution is obtained for the steady MHD plane orthogonal stagnation-point flow of a homogeneous, incompressible, electrically conducting micropolar fluid over a rigid uncharged dielectric at rest. The space is permeated by a not uniform external magnetic field $\mathbf{H}_e$ and the total magnetic field $\mathbf{H}$ in the fluid is parallel to the velocity at infinity. The results obtained reveal many interesting behaviours of the flow and of the total magnetic field in the fluid and in the dielectric. In particular, the thickness of the layer where the viscosity appears depends on the strength of the magnetic field. The effects of the magnetic field on the velocity and on the microrotation profiles are presented graphically and discussed.

Keywords: Micropolar fluids, MHD flow, orthogonal stagnation-point flow, numerical solutions.
2010 MSC: 76W05, 76D10.

Email addresses: brs@unife.it (Alessandra Borrelli), gntgli@unife.it (Giulia Giantesio), pat@unife.it (Maria Cristina Patria)

MHD orthogonal stagnation-point flow of a micropolar fluid with the magnetic field parallel to the velocity at infinity

Alessandra Borrelli

Dipartimento di Matematica e Informatica, Università di Ferrara, via Machiavelli 35, 44121 Ferrara Italy

Giulia Giantesio

Dipartimento di Matematica e Informatica, Università di Ferrara, via Machiavelli 35, 44121 Ferrara Italy

Maria Cristina Patria

Dipartimento di Matematica e Informatica, Università di Ferrara, via Machiavelli 35, 44121 Ferrara Italy

---

Nomenclature

a	positive constant ($[t^{-1}]$)
c_1, c_2, c_3	dimensionless positive micropolar contants
$\mathbf{E}$	electric field ($[lMt^{-3}i^{-1}]$)
$(\mathbf{e}_1, \mathbf{e}_2, \mathbf{e}_3)$	canonical base of $\mathbb{R}^3$
$\mathbf{H}$	total magnetic field ($[l^{-1}i]$)
$\mathbf{H}_e$	external magnetic field
H_∞	costant ($[l^{-2}i]$)
I	microinertia coefficient ($[l^2]$)
p	pressure ($[l^{-1}Mt^{-2}]$)
p_0	pressure at the stagnation-point
R_m	magnetic Reynolds number, dimensionless
$\mathbf{v}$	velocity field ($[lt^{-1}]$)
$\mathbf{w}$	microrotation field ($[t^{-1}]$)

Greek symbols

Email addresses: brs@unife.it (Alessandra Borrelli), gntgli@unife.it (Giulia Giantesio), pat@unife.it (Maria Cristina Patria)

β_m	dimensionless constant
η	dimensionless spatial variable
η_e	electrical permettivity ($\eta_e = (\mu_e \sigma_e)^{-1}$) ($[l^2 t^{-1}]$)
λ, λ_0	microrotation positive constants ($[l^4 t^{-1}]$)
μ_e	magnetic permeability ($[lMt^{-2} i^{-2}]$)
ν	Newtonian viscosity coefficient ($[l^2 t^{-1}]$)
ν_r	microrotation viscosity coefficient ($[l^2 t^{-1}]$))
ρ	mass density ($[l^{-3} M]$)
σ_e	electrical conductivity ($[l^{-3} M^{-1} t^3 i^2]$)
φ, Φ, Ψ	dimensionless unknown functions describing velocity, microrotation, magnetic field

1. Introduction

This paper is devoted to the MHD orthogonal stagnation-point flow of a micropolar fluid under the influence of an external not uniform magnetic field. The micropolar fluids are a model of Non-Newtonian fluids introduced by Eringen ([1]). This model describes fluids consisting of rigid randomly oriented particles suspended in a viscous medium which have an intrinsic rotational micromotion (for example biological fluids in thin vessels, polymeric suspensions, slurries, colloidal fluids). Extensive reviews of the theory and its applications can be found in [2] and [3]. In recent years a vast amount of literature concerning analytical solutions of flow of a micropolar fluid is available ([4], [5], [6], [7]); moreover many papers about applications and numerical simulations have been published ([8], [9], [10], [11], [12], [13], [14], [15], [16], [17]).
Orthogonal stagnation-point flow appears for example when a jet of fluid impinges orthogonally on a solid obstacle. From a mathematical point of view, this motion represents one of the oldest examples of similarity solutions of the PDEs that govern the flow.
The steady two-dimensional orthogonal stagnation-point flow of a Newtonian fluid has been studied starting from the work of Hiemenz ([18]). The same flow was treated by Guram and Smith ([19]) in the micropolar case. Previously Ahmadi ([20]) obtained self-similar solutions of the boundary layer equations for micropolar flow imposing restrictive conditions on the material parameters which make the equations to contain only one parameter and not three as in the general case here considered.
In many physical and engineering problems it is important to study the influence of an external electromagnetic field on such a flow from both a theoretical and a practical point of view.

In this paper we extend the results of [21] about Newtonian fluids to incompressible homogeneous micropolar fluids. Actually, we consider the orthogonal stagnation-point flow of such a fluid filling the half-space $x_2 \geq 0$ when the total magnetic field $\mathbf{H}$ is parallel to the velocity at infinity. We underline that $\mathbf{H}$ is not uniform and it depends on a sufficiently regular unknown function $h = h(x_2)$. We assume that an external magnetic field $\mathbf{H_e}$ permeates the whole space and

the external electric field is absent.
The region where the fluid motion occurs is bordered by the boundary of a solid obstacle which is a rigid uncharged dielectric at rest.
As it is reasonable from the physical point of view, we first consider an inviscid fluid and the situation of the solid.
As far as the electromagnetic field in the solid $(\mathbf{H_s}, \mathbf{E_s})$ is concerned, of course $\mathbf{E_s}$ is zero and we determine $\mathbf{H_s}$ by asking that the non-degenerate field lines of $\mathbf{H_s}$ tend to $x_2 = 0$ as x_1 goes to infinity. We find that $(\mathbf{H}, \mathbf{E}) = (\mathbf{H}_e, \mathbf{0})$ and the pressure field is not modified by the presence of $\mathbf{H}$.
We then analyze the same problem for a Newtonian fluid. The results here presented extend the existing ones in [21], because there the Authors didn't explain properly the physics of the problem and didn't take into consideration the behaviour of the solution, the influence of the parameters on the motion and the thickness of the boundary layer where the effect of the viscosity occurs.

These preliminary considerations allow us to develop exhaustively the problem for a micropolar fluid. We find that the pressure field and the flow depend on $h(x_2)$. $\mathbf{H}$, $\mathbf{v}$ and the microrotation $\mathbf{w}$ satisfy an ordinary differential boundary value problem which depends on two parameters R_m and β_m. R_m is the Reynolds number, while β_m is a measure of the strength of the applied magnetic field.
For both fluids we find that the thickness of the boundary layer depends on R_m and β_m. More precisely, it increases as β_m increases, while it decreases as R_m increases.
Some numerical examples and pictures are given in order to illustrate the effects due to the magnetic field and the behaviour of the solution. These numerical results are obtained by using the MATLAB routine bvp4c. Such a routine is a finite difference code that implements the three-stage Lobatto IIIa formula. This is a collocation formula and here the collocation polynomial provides a C^1-continuous solution that is fourth-order accurate uniformly in $[0, 5]$. Mesh selection and error control are based on the residual of the continuous solution. We set the relative and the absolute tolerance equal to 10^{-7}. The method was used and described in [22].

The paper is organized in this way:
Section 2 deals with the situation of the solid obstacle and of the inviscid fluid. The study of the inviscid flow is important because we require that the pressure and the flow of a viscous stagnation-point flow approach the pressure and the flow of an inviscid fluid far from the obstacle. This condition is deduced from the physical experience. The result obtained for the electromagnetic field in the solid is independent of the kind of fluid.
Section 3 is devoted to the Newtonian fluids. The graphics and the Table extend the results contained in [21].
In Section 4 we examine the same flow of a micropolar fluid.
Section 5 summarizes the conclusions.

2. Preliminaries

We examine the steady MHD plane orthogonal stagnation-point flow under an hypothesis assuring that the magnetic field is parallel to the flow at infinity. The wall towards which the fluid is pointed is the boundary of a solid which is a rigid uncharged dielectric at rest. This problem has been introduced in [21] for a Newtonian fluid, but the Authors didn't explain properly the physics of the problem and didn't consider the thickness of the boundary layer, the behaviour of the solution and the influence of the parameters on the motion. The aim of this paper is to develop this topic for a micropolar fluid. For the sake of completeness and to clarify the physics of the problem we will first study the problem for an inviscid and a Newtonian fluid.

Let us consider the steady plane MHD flow of a homogeneous, incompressible, electrically conducting inviscid fluid near a stagnation point filling the half-space $\mathcal{S}$ (see Figure 1), given by

$$\mathcal{S} = \{(x_1, x_2, x_3) \in \mathbb{R}^3 : (x_1, x_3) \in \mathbb{R}^2, x_2 > 0\}. \tag{1}$$

The coordinate axes are fixed in order to have that the stagnation-point coincides with the origin and we denote by $(\mathbf{e}_1, \mathbf{e}_2, \mathbf{e}_3)$ the canonical base of $\mathbb{R}^3$. $\partial\mathcal{S}$, i.e. the plane $x_2 = 0$, is the boundary of a solid which is a rigid uncharged dielectric at rest occupying $\mathcal{S}^-$ given by

$$\mathcal{S}^- = \{(x_1, x_2, x_3) \in \mathbb{R}^3 : (x_1, x_3) \in \mathbb{R}^2, x_2 < 0\}. \tag{2}$$

We are interested in the orthogonal plane stagnation-point flow so that

$$v_1 = ax_1, \quad v_2 = -ax_2, \quad v_3 = 0, \qquad x_1 \in \mathbb{R}, \quad x_2 \in \mathbb{R}^+, \tag{3}$$

with a positive constant.

The equations governing such a flow in the absence of external mechanical body forces and free electric charges are

$$\begin{aligned}
&\rho\mathbf{v} \cdot \nabla\mathbf{v} = -\nabla p + \mu_e(\nabla \times \mathbf{H}) \times \mathbf{H},\\
&\nabla \cdot \mathbf{v} = 0,\\
&\nabla \times \mathbf{H} = \sigma_e(\mathbf{E} + \mu_e\mathbf{v} \times \mathbf{H}),\\
&\nabla \times \mathbf{E} = \mathbf{0}, \quad \nabla \cdot \mathbf{E} = 0, \quad \nabla \cdot \mathbf{H} = 0, \qquad \text{in } \mathcal{S}
\end{aligned} \tag{4}$$

where $\mathbf{v}$ is the velocity field, p is the pressure, $\mathbf{E}$ and $\mathbf{H}$ are the electric and magnetic fields, respectively, ρ is the mass density (constant > 0), μ_e is the magnetic permeability, σ_e is the electrical conductivity ($\mu_e, \sigma_e =$ constants > 0). As usual, we impose the no-penetration condition to the velocity field and we suppose that the tangential components of $\mathbf{H}$ and $\mathbf{E}$ and the normal components of $\mathbf{B} = \mu_e\,\mathbf{H}$ and $\mathbf{D} = \epsilon\,\mathbf{E}$ ($\epsilon =$ dielectric constant) are continuous across the

plane $x_2 = 0$.
We suppose that the external magnetic field

$$\mathbf{H}_e = H_\infty(x_1\mathbf{e}_1 - x_2\mathbf{e}_2),\ H_\infty = \text{constant},\ x_1 \in \mathbb{R},\ x_2 \in \mathbb{R},$$

permeates the whole physical space and that the external electric field $\mathbf{E}_e$ is absent.

Remark 1. As it is easy to verify, the field lines of $\mathbf{H}_e$ have the following parametric equations

$$\begin{aligned} x_1 &= A_1 e^{H_\infty s}, \\ x_2 &= A_2 e^{-H_\infty s}, \qquad s \in \mathbb{R}, \end{aligned} \tag{5}$$

where $A_1,\ A_2$ are arbitrary constants. These field lines degenerate if at least one of the two constants $A_1,\ A_2$ vanishes. Otherwise they are the hyperbolas

$$x_1 x_2 = A_1 A_2.$$

We remark that these hyperbolas tend to $x_2 = 0$ as $|x_1| \to +\infty$.

We assume that the total magnetic fields in the fluid and in the solid have the following form

$$\begin{aligned} &\mathbf{H} = H_\infty[x_1 h'(x_2)\mathbf{e}_1 - h(x_2)\mathbf{e}_2],\ x_2 \geq 0, \quad \text{and} \\ &\mathbf{H}_s = H_\infty[x_1 h_s'(x_2)\mathbf{e}_1 - h_s(x_2)\mathbf{e}_2],\ x_2 \leq 0, \end{aligned} \tag{6}$$

respectively, where h, h_s are sufficiently regular unknown functions to be determined ($h,\ h_s \in C^2(\mathbb{R}^+)$).
We ask that $\mathbf{H}$ tends to $\mathbf{H}_e$ as $x_2 \to +\infty$ so that $\mathbf{H}$ is parallel to $\mathbf{v}$ at infinity and

$$\lim_{x_2 \to +\infty} h'(x_2) = 1,\ \lim_{x_2 \to +\infty}[h(x_2) - x_2] = 0. \tag{7}$$

Moreover we suppose that

(i) $\mathbf{H}_s$ is not uniform;

(ii) the non-degenerate field lines of $\mathbf{H}_s$ tend to $x_2 = 0$ as $|x_1| \to +\infty$.

Now our aim is to prove the following theorem

Theorem 2. *If the solid which occupies $\mathcal{S}^-$ is a rigid uncharged dielectric at rest and $\mathbf{H}_s$ of the form $(6)_1$ satisfies (i) and (ii), then the magnetic field $\mathbf{H}_s$ is given by*

$$\mathbf{H}_s = H_\infty h'(0)(x_1\mathbf{e}_1 - x_2\mathbf{e}_2),\ x_2 \leq 0, \tag{8}$$

where $h(x_2)$ is the function in $(6)_1$.

Proof:
Since the solid is an uncharged dielectric, it holds

$$\nabla \times \mathbf{H}_s = \mathbf{0}, \quad \text{in } \mathcal{S}^-,$$

from which we get

$$h_s(x_2) = C_1 x_2 + C_2, \quad x_2 \leq 0, \tag{9}$$

where $C_1,\ C_2 \in \mathbb{R}$.
By virtue of the continuity of the tangential components of the magnetic field across the plane $x_2 = 0$, since in $\mathcal{S}$ the total magnetic field is $(6)_1$, we find

$$C_1 = h'(0),$$

so that

$$\mathbf{H}_s = H_\infty \{h'(0) x_1 \mathbf{e}_1 - [h'(0) x_2 + C_2]\mathbf{e}_2\}. \tag{10}$$

We remark that if $h'(0) = 0$, then $\mathbf{H_s}$ is uniform which contradicts hypothesis (i).
Hence $h'(0) \neq 0$ and the magnetic field lines in the solid are

$$\begin{aligned} x_1 &= B_1 e^{H_\infty h'(0)\lambda}, \\ x_2 &= B_2 e^{-H_\infty h'(0)\lambda} - \frac{C_2}{h'(0)}, \qquad\qquad x_2 \leq 0,\ B_1,\ B_2 \in \mathbb{R}. \end{aligned} \tag{11}$$

The non-degenerate field lines are the curves

$$x_1 x_2 = B_1 B_2 - \frac{C_2}{h'(0)} x_1, \qquad x_2 \leq 0,\ B_1, B_2 \neq 0. \tag{12}$$

The curves in (12) tend to $x_2 = 0$ as $|x_1| \to +\infty$ if, and only if,

$$C_2 = 0,$$

from which we get the assertion.

Remark 3. Of course $\mathbf{E_s} = \mathbf{0}$ in $\mathcal{S}^-$.

Remark 4. We underline that Theorem 2 holds even if $\mathcal{S}$ is occupied by a viscous fluid (Newtonian, micropolar and so on) for which $\mathbf{H}$ has the form $(6)_1$.

We now consider the inviscid fluid filling the half-space $\mathcal{S}$. Since $\mathcal{S}$ is in contact with the solid through the plane $x_2 = 0$, from the continuity of the normal component of $\mathbf{B}$ and from $(6)_1$ and (8) we deduce

$$h(0) = 0. \tag{13}$$

Our purpose is now to determine $(p,\ \mathbf{H},\ \mathbf{E})$ solution of (4) in $\mathcal{S}$ with $\mathbf{v}$ given by (3) such that $\mathbf{H}$ tends to $\mathbf{H}_e$ as x_2 goes to infinity so that

$$\mathbf{v} \times \mathbf{H} = \mathbf{0} \text{ at infinity } (x_2 \to +\infty). \tag{14}$$

Let the electric field $\mathbf{E}$ be in the form

$$\mathbf{E} = E_1\mathbf{e}_1 + E_2\mathbf{e}_2 + E_3\mathbf{e}_3.$$

The boundary conditions and the Remark 3 require that

$$E_1 = 0,\ E_3 = 0 \ \text{ at } \ x_2 = 0. \tag{15}$$

From $(4)_4$ follows that

$$\mathbf{E} = -\nabla\psi,$$

where ψ is the electrostatic scalar potential.

Moreover, $(4)_3$ provides $E_1 = E_2 = 0$ so that $\psi = \psi(x_3)$ and

$$\frac{d\psi}{dx_3}(x_3) = \frac{H_\infty}{\sigma_e}x_1\{h''(x_2) + \sigma_e\mu_e a[h'(x_2)x_2 - h(x_2)]\} = -E_3. \tag{16}$$

Further from $(15)_2$, we get $\mathbf{E} = \mathbf{0}$ and

$$h''(x_2) + \sigma_e\mu_e a[h'(x_2)x_2 - h(x_2)] = 0. \tag{17}$$

Equation (17) with the boundary conditions (13) and $(7)_1$ has the unique solution $h(x_2) = x_2$. This furnishes

$$\mathbf{H} = \mathbf{H}_e = H_\infty(x_1\mathbf{e}_1 - x_2\mathbf{e}_2).$$

Since $\nabla \times \mathbf{H} = \mathbf{0}$, from $(4)_1$ follows that the pressure field is not modified by the presence of the magnetic field.
We summarize the results obtained for the inviscid fluid in the following theorem.

Theorem 5. *Let us consider the steady orthogonal stagnation-point flow of a homogeneous, incompressible, electrically conducting inviscid fluid that occupies the half-space $\mathcal{S}$ and is embedded in the external electromagnetic field $\mathbf{H}_e = H_\infty(x_1\mathbf{e}_1 - x_2\mathbf{e}_2)$, $\mathbf{E}_e = \mathbf{0}$. If the total magnetic field in the fluid of the form $(6)_1$ satisfies (7) and the total magnetic field in the solid is given by (8), then*

$$\mathbf{E} = \mathbf{0}, \quad \mathbf{H} = \mathbf{H}_e,$$

$$p = -\frac{1}{2}\rho a^2(x_1^2 + x_2^2) + p_0, \qquad x_1 \in \mathbb{R}, \quad x_2 \in \mathbb{R}^+, p_0 \in \mathbb{R}. \tag{18}$$

where $p_0 \in \mathbb{R}$ is the pressure at the stagnation point.

Remark 6. The previous result states that $\mathbf{H} = \mathbf{H_s} = \mathbf{H_e}$, i.e. the presence of the solid doesn't influence the total magnetic field in the fluid which coincides with the external magnetic field.

In order to study the influence of $\mathbf{H}_e$ on the steady orthogonal plane stagnation-point flow for viscous fluids, it is convenient to suppose that the inviscid fluid orthogonally impinges on the flat plane $x_2 = A$ where A is a constant so that

$$\mathbf{v} = a[x_1\mathbf{e}_1 - (x_2 - A)\mathbf{e}_2], \quad \mathbf{H}_e = H_\infty[x_1\mathbf{e}_1 - (x_2 - A)\mathbf{e}_2] \qquad x_1 \in \mathbb{R}, \quad x_2 \geq A,$$
$$\mathbf{H} \to H_\infty[x_1\mathbf{e}_1 - (x_2 - A)\mathbf{e}_2] \quad \text{as } x_2 \to +\infty. \tag{19}$$

In such a way the stagnation point is not $(0, 0)$ but $(0, A)$, the streamlines and the field lines of $\mathbf{H}_e$ are the hyperbolas whose asymptotes are $x_1 = 0$ and $x_2 = A$ and all previous arguments continue to hold by replacing x_2 by $x_2 - A$. Therefore in this case

$$\mathbf{H} = H_\infty[x_1\mathbf{e}_1 - (x_2 - A)\mathbf{e}_2], \quad p = -\frac{1}{2}\rho a^2\left[x_1^2 + (x_2 - A)^2\right] + p_0. \tag{20}$$

3. Newtonian fluids

Let us consider now the previous problem for a homogeneous, incompressible, electrically conducting Newtonian fluid. The equations governing such a flow in the absence of external mechanical body forces and free electric charges are

$$\begin{aligned}
&\mathbf{v} \cdot \nabla\mathbf{v} = -\frac{1}{\rho}\nabla p + \nu\triangle\mathbf{v} + \frac{\mu_e}{\rho}(\nabla \times \mathbf{H}) \times \mathbf{H},\\
&\nabla \cdot \mathbf{v} = 0,\\
&\nabla \times \mathbf{H} = \sigma_e(\mathbf{E} + \mu_e\mathbf{v} \times \mathbf{H}),\\
&\nabla \times \mathbf{E} = \mathbf{0}, \quad \nabla \cdot \mathbf{E} = 0, \quad \nabla \cdot \mathbf{H} = 0, \qquad\qquad \text{in } \mathcal{S}
\end{aligned} \tag{21}$$

where ν is the kinematic viscosity.
As far as boundary conditions are concerned, we modify only the condition for $\mathbf{v}$, assuming the no-slip boundary condition

$$\mathbf{v}|_{x_2=0} = \mathbf{0}. \tag{22}$$

Since we are interested in the orthogonal plane stagnation-point flow we suppose

$$v_1 = ax_1f'(x_2), \quad v_2 = -af(x_2), \quad v_3 = 0, \qquad x_1 \in \mathbb{R}, \quad x_2 \in \mathbb{R}^+, \tag{23}$$

with f sufficiently regular unknown function ($f \in C^3(\mathbb{R}^+)$).
The condition (22) supplies

$$f(0) = 0, \quad f'(0) = 0. \tag{24}$$

As for the inviscid fluid, we assume that the external magnetic field

$$\mathbf{H}_e = H_\infty(x_1\mathbf{e}_1 - x_2\mathbf{e}_2)$$

permeates the whole physical space and that the external electric field $\mathbf{E}_e = \mathbf{0}$. Further we suppose that the total magnetic field in the fluid is given by $(6)_1$ where h is a sufficiently regular unknown function ($h \in C^2(\mathbb{R}^+)$) that by virtue of (8) satisfies condition (13).
Moreover, we impose the following

Condition P. *The MHD orthogonal stagnation-point flow of a viscous fluid approaches at infinity the flow of an inviscid fluid whose velocity, magnetic field and pressure are given by* $(19)_1$,$(20)_1$ *and* $(20)_2$*, respectively.*

Therefore to (21) we must append the following conditions

$$\lim_{x_2\to+\infty} f'(x_2) = 1, \quad \lim_{x_2\to+\infty} h'(x_2) = 1. \tag{25}$$

The asymptotic behaviour of f and h at infinity is related to the constant A in (19) in the following way:

$$\lim_{x_2\to+\infty}[f(x_2) - x_2] = -A, \quad \lim_{x_2\to+\infty}[h(x_2) - x_2] = -A, \tag{26}$$

so that

$$\mathbf{v}\times\mathbf{H} = \mathbf{0} \text{ at infinity.} \tag{27}$$

We underline that the constant A is not a priori assigned but its value can be computed as part of the solution of the problem.

Our aim is now to determine ($p,\ f,\ \mathbf{H},\ \mathbf{E}$) solution in $\mathcal{S}$ of (21) with $\mathbf{v},\ \mathbf{H}$ given by (23), $(6)_1$, respectively, such that Condition P holds.

As for the inviscid fluid, the electric field $\mathbf{E}$ satisfies the boundary conditions

$$E_1 = 0,\ E_3 = 0 \ \text{ at } \ x_2 = 0. \tag{28}$$

By using the same arguments as in previous section, we get $\mathbf{E} = \mathbf{0}$ in $\mathcal{S}$ and

$$h''(x_2) + \sigma_e\mu_e a[f(x_2)h'(x_2) - h(x_2)f'(x_2)] = 0. \tag{29}$$

We now proceed in order to determine f and p. If we substitute (23) into $(21)_1$, then in components we obtain

$$\begin{aligned}
&ax_1\left[\nu f''' + aff'' - af'^2 - \frac{\mu_e}{\rho a}H_\infty^2 hh''\right] = \frac{1}{\rho}\frac{\partial p}{\partial x_1},\\
&\nu a f'' + a^2 ff' + \frac{\mu_e}{\rho}H_\infty^2 x_1^2 h'h'' = -\frac{1}{\rho}\frac{\partial p}{\partial x_2},\\
&\frac{\partial p}{\partial x_3} = 0 \quad\Rightarrow\quad p = p(x_1, x_2).
\end{aligned} \tag{30}$$

By integrating $(30)_2$, we find

$$p = -\rho\frac{a^2}{2}f^2(x_2) - \rho a\nu f'(x_2) - \mu_e\frac{H_\infty^2}{2}x_1^2 h'^2(x_2) + P(x_1),$$

where the function $P(x_1)$ is determined supposing that, far from the wall, the pressure p has the same behaviour as for an inviscid fluid, whose velocity is given by (19) and the magnetic field and the pressure are given by (20).
Therefore, by virtue of (25) and (26), we get

$$P(x_1) = -\rho\frac{a^2}{2}x_1^2 + \mu_e\frac{H_\infty^2}{2}x_1^2 + p_0^*,$$

where p_0^* is a suitable constant.
Finally, the pressure field assumes the form

$$p = -\rho\frac{a^2}{2}[x_1^2 + f^2(x_2)] - \rho a\nu f'(x_2) - \mu_e\frac{H_\infty^2}{2}x_1^2[h'^2(x_2) - 1] + p_0, \tag{31}$$

where the constant p_0 is the pressure at the origin.
In consideration of (31), from $(30)_1$ we obtain the ordinary differential equation

$$\frac{\nu}{a}f''' + ff'' - f'^2 + 1 - \frac{\mu_e}{\rho}\frac{H_\infty^2}{a^2}[hh'' - h'^2 + 1] = 0. \tag{32}$$

We can now summarize our results in the following

Theorem 7. *Let us consider a homogeneous, incompressible, electrically conducting Newtonian fluid that occupies the half-space $\mathcal{S}$ and is embedded in the external electromagnetic field $\mathbf{H}_e = H_\infty(x_1\mathbf{e}_1 - x_2\mathbf{e}_2)$, $\mathbf{E}_e = \mathbf{0}$. If the total magnetic field in the solid is given by* (8)*, then the steady MHD orthogonal plane stagnation-point flow of such a fluid has the form*

$$\begin{aligned}
\mathbf{v} =& ax_1 f'(x_2)\mathbf{e_1} - af(x_2)\mathbf{e_2},\\
\mathbf{H} =& H_\infty[x_1 h'(x_2)\mathbf{e}_1 - h(x_2)\mathbf{e}_2], \quad \mathbf{E} = \mathbf{0},\\
p =& -\rho\frac{a^2}{2}[x_1^2 + f^2(x_2)] - \rho a\nu f'(x_2) - \mu_e\frac{H_\infty^2}{2}x_1^2[h'^2(x_2) - 1] + p_0,\\
& x_1 \in \mathbb{R}, \quad x_2 \in \mathbb{R}^+,
\end{aligned} \tag{33}$$

where (f, h) satisfies the problem (32)*,* (29)*,* (24)*,* (13)*,* (25)*.*

The problem (32), (29), (24), (13), (25) is solved numerically due to its nonlinearity.
From the numerical solution we will see that f and h satisfy (26) and we compute the value of A.

In order to reduce the number of the parameters, it is convenient to write the boundary value problem in Theorem 7 in dimensionless form putting

$$\eta = \sqrt{\frac{a}{\nu}}x_2, \quad \varphi(\eta) = \sqrt{\frac{a}{\nu}}f\left(\sqrt{\frac{\nu}{a}}\eta\right), \quad \Psi(\eta) = \sqrt{\frac{a}{\nu}}h\left(\sqrt{\frac{\nu}{a}}\eta\right). \tag{34}$$

So we can rewrite problem (32), (29), (13), (25) as:

$$\begin{aligned}
&\varphi''' + \varphi\varphi'' - \varphi'^2 + 1 - \beta_m(\Psi\Psi'' - \Psi'^2 + 1) = 0,\\
&\Psi'' + R_m(\varphi\Psi' - \Psi\varphi') = 0,\\
&\varphi(0) = 0,\ \varphi'(0) = 0,\ \Psi(0) = 0,\\
&\lim_{\eta\to+\infty}\varphi'(\eta) = 1,\ \lim_{\eta\to+\infty}\Psi'(\eta) = 1,
\end{aligned} \tag{35}$$

where $\beta_m = \dfrac{\mu_e}{\rho}\dfrac{H_\infty^2}{a^2}$, $R_m = \dfrac{\nu}{\eta_e}$, $(\eta_e = (\sigma_e\mu_e)^{-1})$ is the magnetic Reynolds number.
The previous nonlinear differential problem has been solved numerically by using the bvp4c MATLAB routine.Such a routine is a finite difference code that implements the three-stage Lobatto IIIa formula. This is a collocation formula and here the collocation polynomial provides a C^1-continuous solution that is fourth-order accurate uniformly in $[0, 5]$. Mesh selection and error control are based on the residual of the continuous solution. We set the relative and the absolute tolerance equal to 10^{-7}. The method was used and described in [22]. The values of R_m and β_m are chosen according to [21], where the Authors have already computed the solution but they didn't take into consideration the thickness of the boundary layer, the behaviour of the solution and the influence of the parameters on the motion.

As far as the value of β_m is concerned, we have that β_m has to be less than 1 in order to preserve the parallelism of $\mathbf{H}$ and $\mathbf{v}$ at infinity, as it will be underlined in the sequel.

Further for small values of R_m, equation $(35)_2$ reduces to $\Psi'' \cong 0$, which gives $\Psi \cong \eta$ so that the influence of the external magnetic field on the flow cannot be shown by system (35). In order to remove this difficulty, it is convenient to use the following transformation ([23], [24])

$$\xi = \sqrt{R_m}\eta,\ \ \varphi_*(\xi) = \sqrt{R_m}\varphi(\sqrt{R_m}\xi),\ \ \Psi_*(\eta) = \sqrt{R_m}\Psi(\sqrt{R_m}\xi). \tag{36}$$

From the numerical integration, we will see that

$$\lim_{\eta\to+\infty}\varphi''(\eta) = 0,\ \lim_{\eta\to+\infty}\varphi'(\eta) = 1.$$

Therefore we define:

- $\overline{\eta}_\varphi$ the value of η such that $\varphi'(\overline{\eta}_\varphi) = 0.99$.

Hence if $\eta > \overline{\eta}_\varphi$, then $\varphi \cong \eta - \alpha$, with $\alpha = \sqrt{\dfrac{a}{\nu}}A$.
So the influence of the viscosity appears only in a layer near to the wall whose thickness is $\overline{\eta}_\varphi\sqrt{\dfrac{\nu}{a}}$.
Moreover $\lim_{\eta\to+\infty}\Psi''(\eta) = 0$, $\lim_{\eta\to+\infty}\Psi'(\eta) = 1$. If we define as $\overline{\eta}_\Psi$ the value of η

such that $\Psi'(\overline{\eta}_\Psi) = 0.99$, then we have that for $\eta > \overline{\eta}_\Psi$, $\Psi \cong \eta - \alpha$.
The numerical results show that the values computed of α for φ and Ψ are in good agreement, especially when β_m is small or R_m is big. This fact can be well observed displaying that the velocity and the magnetic field are parallel far from the obstacle, as we will see in the next figures.
The values of α, $\varphi''(0)$, $\Psi'(0)$ depend on R_m and β_m, as we can see from Table 1.
Table 1 has been obtained for small values of R_m recomputing the corresponding values of η, φ and Ψ after using transformation (36).
We see that α increases, while $\varphi''(0)$ and $\Psi'(0)$ decrease as β_m is increased from 0. Further α, $\varphi''(0)$ and $\Psi'(0)$ decrease as R_m increases.
We remark that $\Psi'(0) \neq 0$ according to hypothesis (i) of Theorem 2.
In Figure 2_1 there are the profiles $\varphi, \varphi', \varphi''$ for $R_m = 1$ and $\beta_m = 0.5$, while Figure 2_2 shows the behaviour of Ψ, Ψ' for the same values of R_m and β_m.
We have plotted the profiles of $\varphi, \varphi', \varphi'', \Psi, \Psi'$ only for $R_m = 1$ and $\beta_m = 0.5$ because they have an analogous trend for $R_m \neq 1$ and $\beta_m \neq 0.5$.
Table 1 underlines that the thickness of the boundary layer depends on R_m and β_m. More precisely, it increases when β_m increases (as is easy to see in Figure 3_1). This behaviour is not surprising because β_m is a measure of the strength of the applied magnetic field and as it is underlined in [21] when the magnetic field is strong the disturbances are no longer contained within a boundary layer along the wall. This means that boundary conditions can no longer be prescribed at infinity. In particular, in [21] it is proved that in a perfectly conducting fluid the displacement thickness becomes infinite as β_m goes to 1^-.

As far as the dependence of the thickness of the boundary layer on R_m is concerned, it decreases when R_m increases (as is easy to see in Figure 3_2). This result is standard in Magnetohydrodynamic.

Finally, we display the streamlines of the flow in Figure 4. As is easily seen from the figures, the flow and the magnetic field are completely overlapped far from the obstacle and the more R_m increases the more the two lines coincide.

4. Micropolar fluids

Consider now the steady two-dimensional MHD orthogonal stagnation-point flow of a homogeneous, incompressible, electrically conducting micropolar fluid towards a flat surface coinciding with the plane $x_2 = 0$, the flow being confined to the half-space $\mathcal{S}$, having equation (1).
In the absence of external mechanical body forces, body couples and free electric

charges, the MHD equations for such a fluid are

$$\begin{aligned}
&\mathbf{v}\cdot\nabla\mathbf{v} = -\frac{1}{\rho}\nabla p + (\nu+\nu_r)\triangle\mathbf{v} + 2\nu_r(\nabla\times\mathbf{w}) + \frac{\mu_e}{\rho}(\nabla\times\mathbf{H})\times\mathbf{H},\\
&\nabla\cdot\mathbf{v} = 0,\\
&I\mathbf{v}\cdot\nabla\mathbf{w} = \lambda\triangle\mathbf{w} + \lambda_0\nabla(\nabla\cdot\mathbf{w}) - 4\nu_r\mathbf{w} + 2\nu_r(\nabla\times\mathbf{v}),\\
&\nabla\times\mathbf{H} = \sigma_e(\mathbf{E}+\mu_e\mathbf{v}\times\mathbf{H}),\\
&\nabla\times\mathbf{E} = \mathbf{0},\quad \nabla\cdot\mathbf{E} = 0,\quad \nabla\cdot\mathbf{H} = 0, \qquad \text{in } \mathcal{S}. \qquad (37)
\end{aligned}$$

where $\mathbf{w}$ is the microrotation field, ν is the kinematic newtonian viscosity coefficient, ν_r is the microrotation viscosity coefficient, λ, λ_0 (positive constants) are material parameters related to the coefficient of angular viscosity and I is the microinertia coefficient.
We notice that in [1], [2], eqs. (37) are slightly different, because they are deduced as a special case of much more general model of microfluids. For the details, we refer to [3], p.23.
As far as the boundary conditions are concerned we prescribe

$$\mathbf{v}|_{x_2=0} = \mathbf{0},\quad \mathbf{w}|_{x_2=0} = \mathbf{0} \text{ (strict adherence condition).} \qquad (38)$$

We search $\mathbf{v}$, $\mathbf{w}$ in the following form

$$\begin{aligned}
&v_1 = ax_1f'(x_2),\quad v_2 = -af(x_2),\quad v_3 = 0,\\
&w_1 = 0,\quad w_2 = 0,\quad w_3 = x_1F(x_2),\qquad x_1\in\mathbb{R},\quad x_2\in\mathbb{R}^+, \qquad (39)
\end{aligned}$$

where f, F are sufficiently regular unknown functions ($f\in C^3(\mathbb{R}^+)$, $F\in C^2(\mathbb{R}^+)$). The conditions (38) supply

$$f(0) = 0,\quad f'(0) = 0,\quad F(0) = 0. \qquad (40)$$

As for the inviscid and Newtonian fluid, we suppose that an external magnetic field

$$\mathbf{H}_e = H_\infty(x_1\mathbf{e}_1 - x_2\mathbf{e}_2)$$

permeates the whole physical space and that the external electric field is absent. Moreover, the total magnetic field in the fluid is taken in the following form

$$\mathbf{H} = H_\infty[x_1h'(x_2)\mathbf{e}_1 - h(x_2)\mathbf{e}_2], \qquad (41)$$

where h is a sufficiently regular unknown function ($h\in C^2(\mathbb{R}^+)$). From Theorem 2 follows that in the solid the total magnetic field has the form $\mathbf{H}_s = H_\infty h'(0)(x_1\mathbf{e}_1 - x_2\mathbf{e}_2)$, which gives the additional condition

$$h(0) = 0. \qquad (42)$$

Moreover, we require that the MHD orthogonal stagnation-point flow satisfies Condition P at infinity.

Therefore to (37) we must also append the following conditions

$$\lim_{x_2\to+\infty} f'(x_2) = 1, \quad \lim_{x_2\to+\infty} F(x_2) = 0, \quad \lim_{x_2\to+\infty} h'(x_2) = 1. \tag{43}$$

Condition $(43)_2$ means that at infinity, $\mathbf{w} = \dfrac{1}{2}\nabla \times \mathbf{v}$, i.e. the micropolar fluid behaves like an inviscid fluid.
The asymptotic behaviour of f and h at infinity is related to x_2 as for the Newtonian case. Hence relation (26) continues to hold, so that

$$\mathbf{v} \times \mathbf{H} = \mathbf{0} \text{ at infinity.} \tag{44}$$

We underline that the constant A is not a priori assigned but its value can be computed as part of the solution of the problem.

Our aim is now to determine $(p,\ f,\ F,\ \mathbf{H},\ \mathbf{E})$ solution in $\mathcal{S}$ of (37) with $\mathbf{v}, \mathbf{w}$ given by (38) such that Condition P holds.

Since $(37)_{3,4,5,6}$ are the same as $(21)_{4,5,6,7}$, $\mathbf{H},\ \mathbf{E}$ depend only on the form of the velocity field, which is the same as that of the Newtonian fluid. Hence, following the arguments of the previous section, we get

$$\mathbf{E} = \mathbf{0}, \quad h''(x_2) + \sigma_e\mu_e a[f(x_2)h'(x_2) - h(x_2)f'(x_2)] = 0. \tag{45}$$

Now we proceed in order to determine $p,\ f,\ F$.
We substitute (39) and (41) in $(37)_{1,3}$ to obtain

$$\begin{aligned}
&ax_1\left[(\nu+\nu_r)f''' + aff'' - af'^2 + \frac{2\nu_r}{a}F' - \frac{\mu_e}{\rho a}H_\infty^2 hh''\right] = \frac{1}{\rho}\frac{\partial p}{\partial x_1},\\
&a(\nu+\nu_r)f'' + a^2 ff' + 2\nu_r F + \frac{\mu_e}{\rho}H_\infty^2 x_1^2 h'h'' = -\frac{1}{\rho}\frac{\partial p}{\partial x_2},\\
&\frac{\partial p}{\partial x_3} = 0 \quad \Rightarrow \quad p = p(x_1, x_2),\\
&\lambda F'' + Ia(F'f - Ff') - 2\nu_r(2F + af'') = 0.
\end{aligned} \tag{46}$$

Then, by integrating $(46)_2$, we find

$$p = -\rho\frac{a^2}{2}f^2(x_2) - \rho a(\nu+\nu_r)f'(x_2) - 2\nu_r\rho\int_0^{x_2} F(s)ds - \mu_e\frac{H_\infty^2}{2}x_1^2 h'^2(x_2) + P(x_1),$$

where the function $P(x_1)$ is determined supposing that, far from the wall, the pressure p has the same behaviour as for an inviscid fluid, whose velocity is given by (19) and the magnetic field and the pressure are given by (20).
Therefore, by virtue of (43), (26) and under the assumption $F \in L^1([0,+\infty))$ we get

$$P(x_1) = -\rho\frac{a^2}{2}x_1^2 + \mu_e\frac{H_\infty^2}{2}x_1^2 + p_0^*,$$

where p_0^* is a suitable constant.
Finally, the pressure field assumes the form

$$p = -\rho\frac{a^2}{2}[x_1^2 + f^2(x_2)] - \rho a(\nu+\nu_r)f'(x_2) - 2\nu_r\rho\int_0^{x_2} F(s)ds$$
$$- \mu_e\frac{H_\infty^2}{2}x_1^2[h'^2(x_2) - 1] + p_0, \tag{47}$$

with p_0 constant.
In consideration of (47), from $(46)_1$ we obtain the ordinary differential equation

$$\frac{\nu+\nu_r}{a}f''' + ff'' - f'^2 + 1 + \frac{2\nu_r}{a^2}F' - \frac{\mu_e}{\rho}\frac{H_\infty^2}{a^2}[hh'' - h'^2 + 1] = 0, \tag{48}$$

together with equations $(46)_4$, $(45)_2$ and the boundary conditions (40), (43) and (42).
Hence we can state

Theorem 8. *Let a homogeneous, incompressible, electrically conducting micropolar fluid occupy the half-space $\mathcal{S}$ and is embedded in the external electromagnetic field $\mathbf{H}_e = H_\infty(x_1\mathbf{e}_1 - x_2\mathbf{e}_2)$, $\mathbf{E}_e = \mathbf{0}$. If the total magnetic field in the solid is given by (8), then the steady MHD orthogonal plane stagnation-point flow of such a fluid has the form*

$$\mathbf{v} = ax_1f'(x_2)\mathbf{e}_1 - af(x_2)\mathbf{e}_2, \quad \mathbf{w} = x_1F(x_2)\mathbf{e}_3,$$
$$\mathbf{H} = H_\infty[x_1h'(x_2)\mathbf{e}_1 - h(x_2)\mathbf{e}_2], \quad \mathbf{E} = \mathbf{0},$$
$$p = -\rho\frac{a^2}{2}[x_1^2 + f^2(x_2)] - \rho a(\nu+\nu_r)f'(x_2)$$
$$- 2\nu_r\rho\int_0^{x_2} F(s)ds - \mu_e\frac{H_\infty^2}{2}x_1^2[h'^2(x_2) - 1] + p_0, \qquad x_1 \in \mathbb{R}, \quad x_2 \in \mathbb{R}^+,$$

where (f, F, h) satisfies the problem (48), $(46)_4$, $(45)_2$ and the boundary conditions (40), (43) and (42), provided $F \in L^1([0, +\infty))$.

Now it is convenient to rewrite the boundary value problem in Theorem 8 in dimensionless form in order to reduce the number of the material parameters. To this end if we use

$$\eta = \sqrt{\frac{a}{\nu+\nu_r}}x_2, \qquad \varphi(\eta) = \sqrt{\frac{a}{\nu+\nu_r}}f\left(\sqrt{\frac{\nu+\nu_r}{a}}\eta\right),$$
$$\Psi(\eta) = \sqrt{\frac{a}{\nu+\nu_r}}h\left(\sqrt{\frac{\nu+\nu_r}{a}}\eta\right), \ \Phi(\eta) = \frac{2\nu_r}{a^2}\sqrt{\frac{a}{\nu+\nu_r}}F\left(\sqrt{\frac{\nu+\nu_r}{a}}\eta\right), \tag{49}$$

then system (48), $(46)_4$ and $(45)_2$ can be written as

$$\begin{aligned}
&\varphi''' + \varphi\varphi'' - \varphi'^2 + 1 + \Phi' - \beta_m(\Psi\Psi'' - \Psi'^2 + 1) = 0,\\
&\Phi'' + c_3\Phi'\varphi - \Phi(c_3\varphi' + c_2) - c_1\varphi'' = 0,\\
&\Psi'' + R_m(\varphi\Psi' - \Psi\varphi') = 0,
\end{aligned} \tag{50}$$

where $c_1,\ c_2,\ c_3, \beta_m, R_m$ are given by

$$\begin{aligned}
&c_1 = \frac{4\nu_r^2}{\lambda a},\quad c_2 = \frac{4\nu_r(\nu+\nu_r)}{\lambda a},\quad c_3 = \frac{I}{\lambda}(\nu+\nu_r),\\
&\beta_m = \frac{\mu_e}{\rho}\frac{H_\infty^2}{a^2},\quad R_m = \frac{\nu+\nu_r}{\eta_e}.
\end{aligned} \tag{51}$$

The boundary conditions (40), (43) and (42) in dimensionless form become:

$$\begin{aligned}
&\varphi(0) = 0,\quad \varphi'(0) = 0,\quad \Phi(0) = 0,\quad \Psi(0) = 0,\\
&\lim_{\eta\to+\infty}\varphi'(\eta) = 1,\quad \lim_{\eta\to+\infty}\Phi(\eta) = 0,\quad \lim_{\eta\to+\infty}\Psi'(\eta) = 1.
\end{aligned} \tag{52}$$

The problem (50), (52) is a nonlinear differential problem that we have solved numerically using the bvp4c MATLAB routine. Such a routine is a finite difference code that implements the three-stage Lobatto IIIa formula. This is a collocation formula and here the collocation polynomial provides a C^1-continuous solution that is fourth-order accurate uniformly in $[0, 5]$. Mesh selection and error control are based on the residual of the continuous solution. We set the relative and the absolute tolerance equal to 10^{-7}. The method was used and described in [22].
The values of c_1, c_2, c_3 are chosen according to [19], while the values of R_m and β_m according to [21] and to the previous section.

As far as the value of β_m is concerned, we recall that β_m has to be less than 1 in order to preserve the parallelism of $\mathbf{H}$ and $\mathbf{v}$ at infinity.
Further for small values of R_m, it is convenient to use a transformation similar to that given by (36).

From the numerical integration, we will see that the solution (φ, Φ, Ψ) of problem (50) satisfies the conditions $(52)_{5,6,7}$; therefore we put:

- $\overline{\eta}_\varphi$ the value of η such that $\varphi'(\overline{\eta}_\varphi) = 0.99$;
- $\overline{\eta}_\Phi$ the value of η such that $\Phi(\overline{\eta}_\Phi) = -0.01$.

Hence if $\eta > \overline{\eta}_\varphi$ then $\varphi \cong \eta - \alpha$, and if $\eta > \overline{\eta}_\Phi$, then $\Phi \cong 0$.
The influence of the viscosity on the velocity and on the microrotation appears only in a layer lining the boundary whose thickness is $\overline{\eta}_\varphi$ for the velocity and $\overline{\eta}_\Phi$ for the microrotation. The thickness δ of the boundary layer for the flow is defined as

$$\delta = \max(\overline{\eta}_\varphi, \overline{\eta}_\Phi).$$

Moreover, as well as in the Newtonian case, $\lim_{\eta\to+\infty} \Psi''(\eta) = 0$, $\lim_{\eta\to+\infty} \Psi'(\eta) = 1$. If we define as $\overline{\eta}_\Psi$ the value of η such that $\Psi'(\overline{\eta}_\Psi) = 0.99$, then we have that for $\eta > \overline{\eta}_\Psi$, $\Psi \cong \eta - \alpha$.
The numerical results show that the values computed of α for φ and Ψ are in good agreement, especially when β_m is small or R_m is big. This fact can be well observed displaying that the velocity and the magnetic field are parallel far from the obstacle, as we will see in the next figures. Table 2 shows the numerical results of the descriptive quantities of problem (50), (52) in dependence of some values of $c_1,\ c_2,\ c_3$, β_m and R_m.

When β_m and R_m are fixed, we see from Table 2 that if we also fix two parameters among c_1, c_2, c_3, then the values of $\alpha,\ \varphi''(0),\ \Phi'(0)$, have the following behaviour :

- they increase as c_2 or c_3 increases;

- they decrease as c_1 increases.

The influence of c_1 appears more considerable also on the quantities quoted in the Table.

Figures from 5 to 7 elucidate the dependence of the functions $\varphi',\ \Phi$ on the parameters $c_1,\ c_2,\ c_3$. We can see that the function which appear most influenced by $c_1,\ c_2,\ c_3$ is Φ, in other words the microrotation. More precisely, the profile of Φ rises as c_3 or c_2 increases and c_1 decreases. As it happened for the descriptive quantities of the motion, c_1 is the parameter that most influences the microrotation.
The function φ' does not show considerable variations as $c_1,\ c_2,\ c_3$ assume different values.

As far as the dependence on R_m and β_m is concerned, we see from Table 2 that:

- if β_m increases, then α and $\Phi'(0)$ increase, while $\varphi''(0)$ and $\Psi'(0)$ decrease;

- if R_m increases, then α, $\varphi''(0)$, $|\Phi'(0)|$ and $\Psi'(0)$ decrease.

In Figure 8_1 we display the profiles $\varphi, \varphi', \varphi''$ when $c_1 = 0.5$, $c_2 = 3.0$, $c_3 = 0.5$, $R_m = 1$ and $\beta_m = 0.5$, while Figure 8_2 shows the behaviour of Φ, Φ' for the same values of the parameters. The behaviour of Ψ, Ψ' is shown in Figure 8_3.

We have plotted the profiles of $\varphi,\ \varphi',\ \varphi'',\ \Phi,\ \Phi',\ \Psi,\ \Psi'$ only for these values of the parameters because they have an analogous behaviour for $c_1 \neq 0.5$, $c_2 \neq 3.0$, $c_3 \neq 0.5$, $R_m \neq 1$ and $\beta_m \neq 0.5$.
Table 2 underlines that the thickness of the boundary layer depends on R_m and β_m. More precisely as in the Newtonian case, it increases as β_m increases (as is easy to see in Figures 9_1 and 9_2) and it decreases as R_m increases (as is easy to see in Figure 9_3 and 9_4).

We underline that the micropolar nature of the fluid reduces all the descriptive quantities of the motion in comparison to those of the Newtonian fluid, especially the thickness of the boundary layer for the velocity.

Finally, we display the streamlines of the flow in Figure 10. As it is easy to see from the figures, the flow and the magnetic field are completely overlapped far from the obstacle and the more R_m increases the more the two lines coincide.

5. Conclusions

In this paper we study the MHD orthogonal stagnation-point flow of a micropolar fluid when the total not uniform magnetic field is parallel to the velocity at infinity. In order to analyze in a complete way the problem, we first examine the same situation for an inviscid and a Newtonian fluid. The region where the fluid motion occurs is bordered by the boundary of a solid obstacle which is a rigid uncharged dielectric at rest. We prove that the total magnetic field in the solid is related to the total magnetic field **H** in the fluid. By means of similarity transformations, we reduce the MHD PDEs to a nonlinear system of ODEs which has been numerically integrated for each model of fluid. The results obtained show that

- The thickness of the boundary layer depends on two parameters: R_m (the magnetic Reynolds number) and β_m (coefficient proportional to the strength of the external magnetic field).
- In the micropolar case, we study the influence of the micropolar constants $c_1,\ c_2,\ c_3$ on the flow.
- The micropolar nature of the fluid reduces all the descriptive quantities of the flow in comparison to the Newtonian case.

Acknoledgement
This work was performed under the auspices of G.N.F.M. of INdAM and supported by Italian MIUR.
The work of one of the authors (G.G.) is part of her Ph.D. Thesis at the University of Ferrara.
The authors are grateful to the referees for the useful and valuable suggestions.

References

[1] A.C. Eringen, Theory of micropolar fluids, J. Math. Mech. 16 (1966) 1-18.

[2] A.C. Eringen, Microcontinuum Field Theories, Vol. $I - II$, Springer-Verlag (2001).

[3] G. Lukaszewicz, Micropolar Fluids Theory and Applications, Birkäuser (1999).

[4] F. Shahzad, M. Sajid, T.Hayat, M. Ayub, Analytic solution for flow a micropolar fluid, Acta Mech. 188 (2006) 93-102.

[5] T.Hayat, T. Javed, Z. Abbas, MHD flow of a micropolar fluid near a stagnation point towards a non-linear streching surface, Nonlinear Analysis: real world application 10 (2009) 1514-1526.

[6] M. Sajid, Z. Abbas, T.Hayat, Homotopy analysis for boundary layer flow of a micropolar fluid thourg a porous channel, Applied Mathematical Modelling 33 (2009) 4120-4125.

[7] F. Xu, Regularity criterion of weak solution for the 3D Magneto-micropolar fluid equations in Besov spaces, Commun Nonlinear Sci Numer Simulat 17 (2012) 2426-2433.

[8] T.Hayat, N. Ali, Z. Abbas, Peristaltic flow of a micropolar fluid in a channel with different wave forms, Physics Letters A 370 (2007) 331-344.

[9] T.Hayat, Z. Abbas, T. Javed, Mixed covection flow of a micropolar fluid over a non-linearly streching shit, Physics Letters A 372 (2008) 637-647.

[10] N. Ali, T.Hayat, Peristaltic flow of a micropolar fluid in a asymetric channel, Computer and mathematics with applications 55 (2008) 589-608.

[11] T.Hayat, N. Ali, Effects of an endoscope on peristaltic flow of a micropolar fluid, Mathematical and computer modelling 48 (2008) 721-733.

[12] M. Sajid, N. Ali, T.Hayat, On exact solutions for thin film flows of a micropolar fluid, Comunications in nonlinear Science and Numerical Simulations 14 (2009) 451-461.

[13] A. Borrelli, G. Giantesio, M. C. Patria, Three-dimensional MHD stagnation point-flow of a Newtonian and a micropolar fluid, IJPAM 73 (2011) 165-188.

[14] A. Borrelli, G. Giantesio, M.C. Patria, MHD oblique stagnation-point flow of a micropolar fluid, Applied Mathematical Modelling 36 (2012) 3949-3970.

[15] A.M. Abd-Alla, G.A. Yahya, S.R. Mahmoud, H.S. Alosaimi, Effect of the rotation, magnetic field and initial stress on peristaltic motion of micropolar fluid, Meccanica 47 (2012) 1455-1465.

[16] M. Ashraf, S. Bashir, Numerical simulation of MHD stagnation point flow and heat transfer of a micropolar fluid towards a heated shrinking sheet, Int. J. Numer. Meth. Fluids 69 (2012) 384-398.

[17] M. A.A. Mahmoud, S. E. Waheed, MHD stagnation point flow of a micropolar fluid towards a moving surface with radiation, Meccanica 47 (2012) 1119-1130.

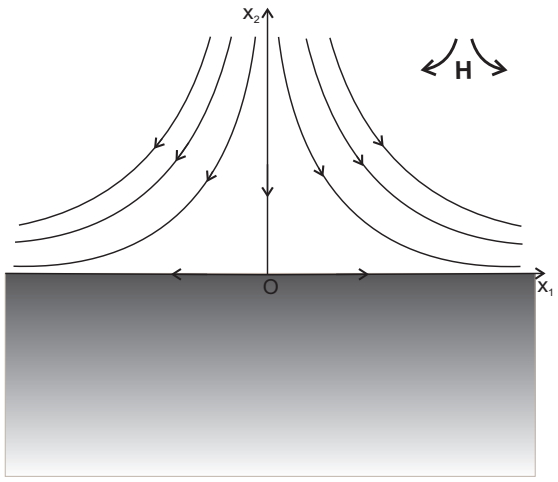

Figure 1: Flow description.

[18] K. Hiemenz, Die Grenzschicht an einem in den gleichformingen Flussigkeitsstrom eingetauchten graden Kreiszylinder, Dinglers Polytech. J. 326 (1911) 321-324.

[19] G.S. Guram, A.C. Smith, Stagnation flows of micropolar fluids with strong and weak interactions, Comp. Maths. with Appls. 6 (1980) 213-233.

[20] G. Ahmadi, Self-Similar solution of imcropressible micropolar boundary layer flow over a semi-infinite plate, Int. F. Engng. Sci. 10 (1976) 639-646.

[21] J.M. Dorrepaal, S. Mosavizadeh, Steady incompressible magnethohydrodynamic flow near a point of reattachment, Phys. Fluids 10 (1998) 1512-1518.

[22] L. F. Shampine, I. Gladwell, S. Thompson, Solving ODEs with MATLAB, Cambridge University Press (2003).

[23] M.B. Glauert, A study of the magnetohydrodynamic boundary layer on a flat plate, J. Fluid Mech. 10 (1961) 276-288.

[24] R.J. Gribben, The Magnetohydrodynamic Boundary Layer in the Presence of a Pressure Gradient, Proc. R. Soc. Lond. A 17 (1965) 123-141.

Table 1: Descriptive quantities of the motion for several values of R_m and β_m.

R_m	β_m	$\varphi''(0)$	$\Psi'(0)$	α	$\overline{\eta}_\varphi$
0.01	0.00	1.2326	0.9273	0.6479	2.3881
	0.20	1.2040	0.9191	0.8021	6.6017
	0.50	1.1435	0.8991	1.2557	19.4174
	0.70	1.0764	0.8733	2.0070	30.1200
	0.90	0.9437	0.8162	4.2495	44.7362
0.1	0.00	1.2326	0.8110	0.6479	2.3802
	0.20	1.1650	0.7922	0.7884	5.2230
	0.50	1.0278	0.7486	1.1879	9.1610
	0.70	0.8877	0.6969	1.8066	12.6325
	0.90	0.6529	0.5994	3.4034	15.2579
1	0.00	1.2326	0.6080	0.6479	2.3806
	0.20	1.1193	0.5812	0.7616	3.1533
	0.50	0.9065	0.5258	1.0511	4.3173
	0.70	0.7189	0.4727	1.4028	4.7799
	0.90	0.4676	0.3976	2.0234	4.9350
100	0.00	1.2326	0.2027	0.6479	2.3806
	0.20	1.1004	0.1895	0.7266	2.6669
	0.50	0.8665	0.1641	0.9234	3.3783
	0.70	0.6686	0.1401	1.1887	4.2186
	0.90	0.3935	0.1010	1.8284	4.8675
1000	0.00	1.2326	0.1003	0.6479	2.3806
	0.20	1.1019	0.0935	0.7247	2.6619
	0.50	0.8704	0.0804	0.9167	3.3621
	0.70	0.6740	0.0683	1.1762	4.1973
	0.90	0.3993	0.0487	1.8071	4.8625

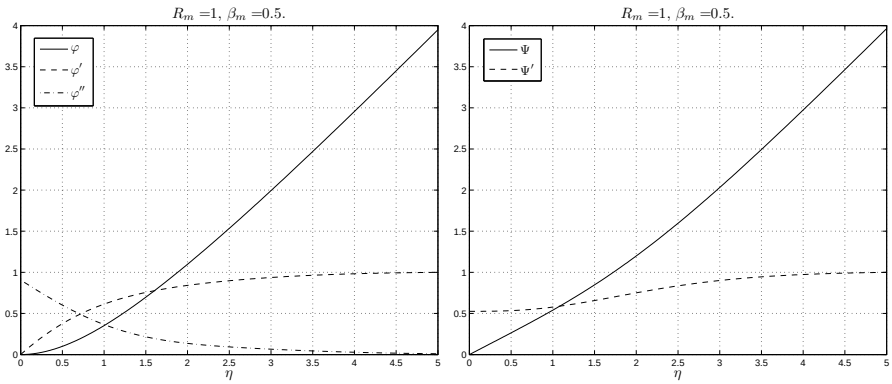

Figure 2: The first figure shows $\varphi, \varphi', \varphi''$ for $R_m = 1$ and $\beta_m = 0.5$, while the second shows Ψ, Ψ' for $R_m = 1$ and $\beta_m = 0.5$.

Table 2: Descriptive quantities of the motion for several values of c_1, c_2, c_3, R_m and β_m.

R_m	β_m	c_1	c_2	c_3	$\varphi''(0)$	$\Psi'(0)$	$\Phi'(0)$	α	$\overline{\eta}_\varphi$	$\overline{\eta}_\Phi$	δ
0.01	0.00	0.10	1.50	0.10	1.2218	0.9275	-0.0532	0.6445	2.3341	0.7669	2.3341
				0.50	1.2231	0.9275	-0.0510	0.6448	2.3508	0.7169	2.3508
			3.00	0.10	1.2250	0.9275	-0.0444	0.6453	2.3508	0.6669	2.3508
				0.50	1.2256	0.9275	-0.0434	0.6454	2.3675	0.6335	2.3675
		0.50	1.50	0.10	1.1780	0.9287	-0.2659	0.6309	2.1340	0.7669	2.1340
				0.50	1.1848	0.9287	-0.2553	0.6321	2.1841	0.7169	2.1841
			3.00	0.10	1.1943	0.9284	-0.2220	0.6350	2.2174	0.6836	2.2174
				0.50	1.1972	0.9284	-0.2173	0.6356	2.2508	0.6502	2.2508
	0.50	0.10	1.50	0.10	1.1335	0.8995	-0.0500	1.2492	19.3731	0.7836	19.3731
				0.50	1.1347	0.8995	-0.0481	1.2496	19.3731	0.7169	19.3731
			3.00	0.10	1.1366	0.8994	-0.0417	1.2508	19.3898	0.6836	19.3898
				0.50	1.1371	0.8994	-0.0408	1.2510	19.3898	0.6502	19.3898
		0.50	1.50	0.10	1.0929	0.9012	-0.2505	1.2227	19.1731	0.7836	19.1731
				0.50	1.0992	0.9011	-0.2409	1.2249	19.1897	0.7336	19.1897
			3.00	0.10	1.1085	0.9007	-0.2085	1.2308	19.2397	0.6836	19.2397
				0.50	1.1111	0.9007	-0.2043	1.2318	19.2564	0.6502	19.2564
1	0.00	0.10	1.50	0.10	1.2218	0.6081	-0.0532	0.6446	2.3258	1.6005	2.3258
				0.50	1.2231	0.6082	-0.0510	0.6448	2.3374	1.3338	2.3374
			3.00	0.10	1.2250	0.6082	-0.0444	0.6453	2.3474	1.0020	2.3474
				0.50	1.2256	0.6083	-0.0434	0.6454	2.3525	0.8469	2.3525
		0.50	1.50	0.10	1.1780	0.6087	-0.2659	0.6310	2.1274	2.9093	2.9093
				0.50	1.1848	0.6093	-0.2553	0.6321	2.1691	2.4325	2.4325
			3.00	0.10	1.1943	0.6092	-0.2220	0.6350	2.2157	2.3441	2.3441
				0.50	1.1972	0.6095	-0.2173	0.6356	2.2391	2.1190	2.2391
	0.50	0.10	1.50	0.10	0.8963	0.5258	-0.0429	1.0463	4.2864	1.8723	4.2864
				0.50	0.8976	0.5260	-0.0413	1.0462	4.2964	1.5038	4.2964
			3.00	0.10	0.8998	0.5260	-0.0350	1.0474	4.2998	0.7469	4.2998
				0.50	0.9003	0.5261	-0.0343	1.0474	4.3031	0.7119	4.3031
		0.50	1.50	0.10	0.8549	0.5255	-0.2141	1.0265	4.1464	3.8913	4.1464
				0.50	0.8616	0.5267	-0.2066	1.0261	4.2031	3.3061	4.2031
			3.00	0.10	0.8727	0.5267	-0.1746	1.0321	4.2281	3.1677	4.2281
				0.50	0.8753	0.5271	-0.1715	1.0321	4.2464	2.8193	4.2464
100	0.00	0.10	1.50	0.10	1.2218	0.2021	-0.0532	0.6446	2.3258	1.6005	2.3258
				0.50	1.2231	0.2023	-0.0510	0.6448	2.3374	1.3338	2.3374
			3.00	0.10	1.2250	0.2024	-0.0444	0.6453	2.3474	1.0020	2.3474
				0.50	1.2256	0.2024	-0.0434	0.6454	2.3525	0.8469	2.3525
		0.50	1.50	0.10	1.1780	0.1999	-0.2659	0.6310	2.1274	2.9093	2.9093
				0.50	1.1848	0.2005	-0.2553	0.6321	2.1691	2.4325	2.4325
			3.00	0.10	1.1943	0.2011	-0.2220	0.6350	2.2157	2.3441	2.3441
				0.50	1.1972	0.2013	-0.2173	0.6356	2.2391	2.1190	2.2391
	0.50	0.10	1.50	0.10	0.8560	0.1635	-0.0439	0.9166	3.2928	1.9590	3.2928
				0.50	0.8574	0.1636	-0.0421	0.9169	3.3178	1.6189	3.3178
			3.00	0.10	0.8595	0.1638	-0.0354	0.9184	3.3311	1.0854	3.3311
				0.50	0.8601	0.1638	-0.0347	0.9186	3.3411	0.7786	3.3411
		0.50	1.50	0.10	0.8126	0.1609	-0.2196	0.8887	2.9460	3.4378	3.4378
				0.50	0.8200	0.1617	-0.2112	0.8907	3.0527	2.9210	3.0527
			3.00	0.10	0.8311	0.1624	-0.1772	0.8984	3.1327	2.8459	3.1327
				0.50	0.8340	0.1627	-0.1738	0.8993	3.1794	2.5792	3.1794

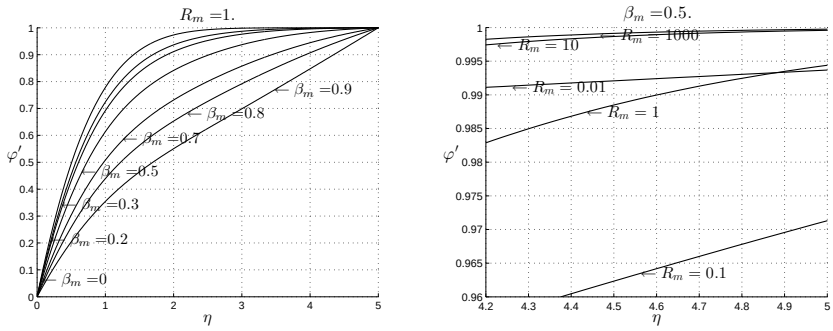

Figure 3: Plots showing φ' for different β_m and R_m, respectively.

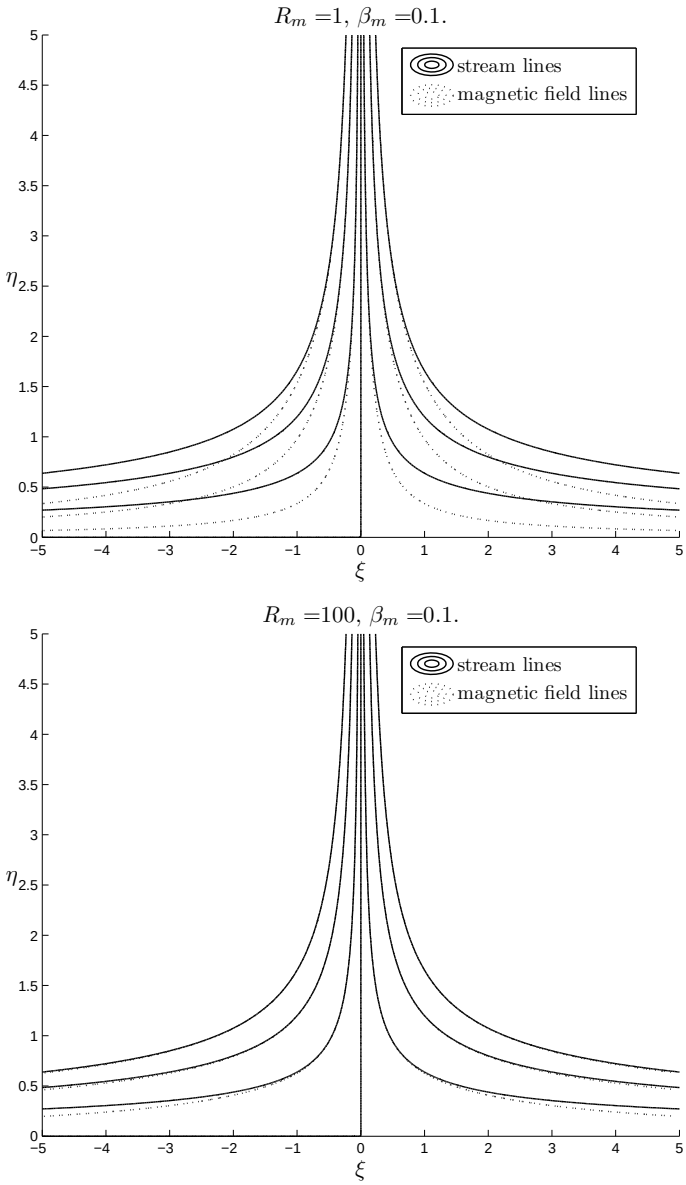

Figure 4: Figures show the streamlines for $\beta_m = 0.1$ and $R_m = 1$ or $R_m = 100$, respectively.

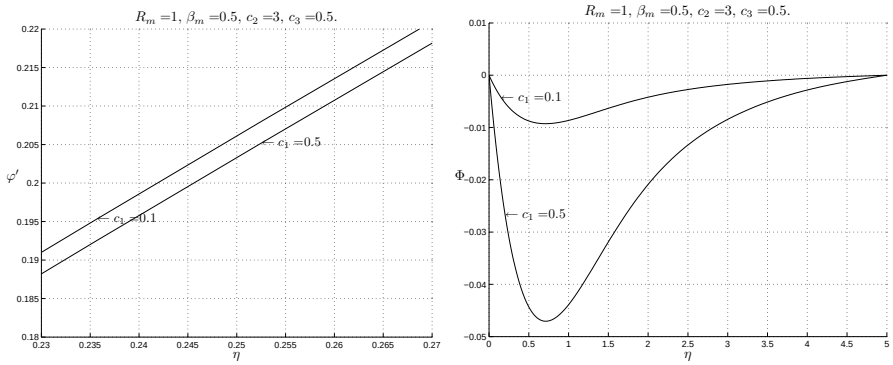

Figure 5: φ', Φ profiles for $R_m = 1,\ \beta_m = 0.5,\ c_2 = 3,\ c_3 = 0.5$ when $c_1 = 0.1$ and $c_1 = 0.5$.

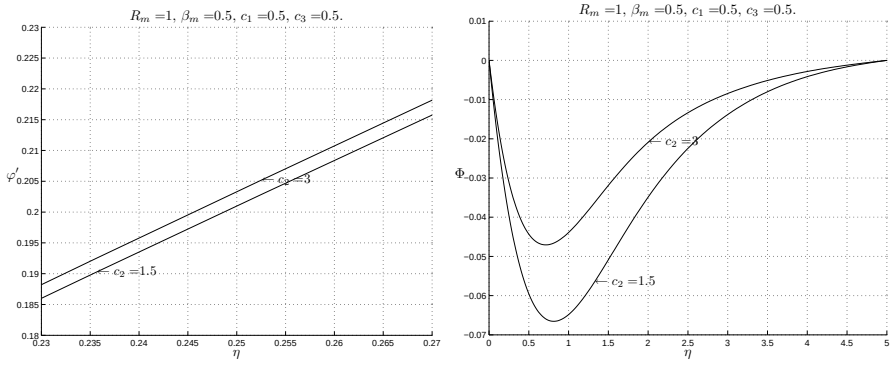

Figure 6: φ', Φ profiles for $R_m = 1,\ \beta_m = 0.5,\ c_1 = 0.5,\ c_3 = 0.5$ when $c_2 = 1.5$ and $c_2 = 3$.

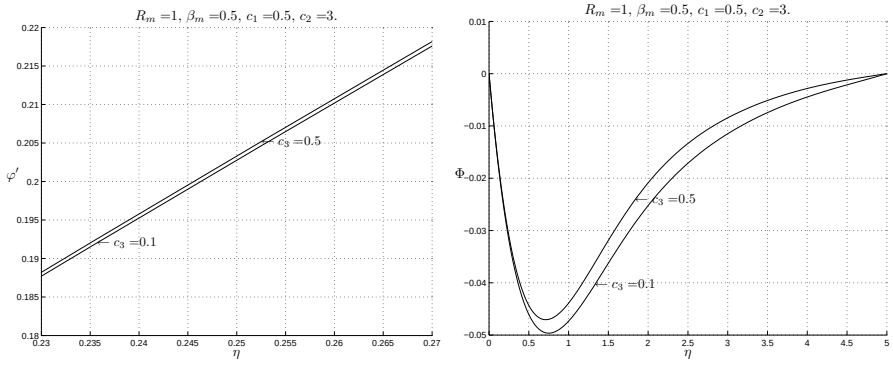

Figure 7: φ', Φ profiles for $R_m = 1,\ \beta_m = 0.5,\ c_1 = 0.5,\ c_2 = 3$ when $c_3 = 0.1$ and $c_3 = 0.5$.

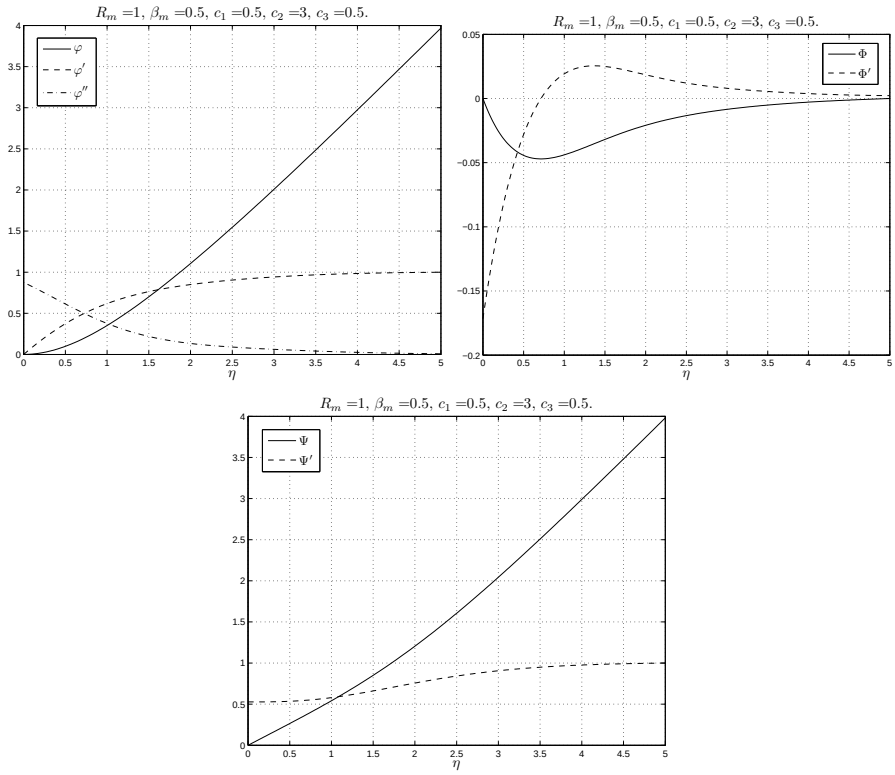

Figure 8: The first figure shows $\varphi, \varphi', \varphi''$, the second Φ, Φ', the third Ψ, Ψ', when $c_1 = 0.5$, $c_2 = 3.0$, $c_3 = 0.5$, $R_m = 1$ and $\beta_m = 0.5$.

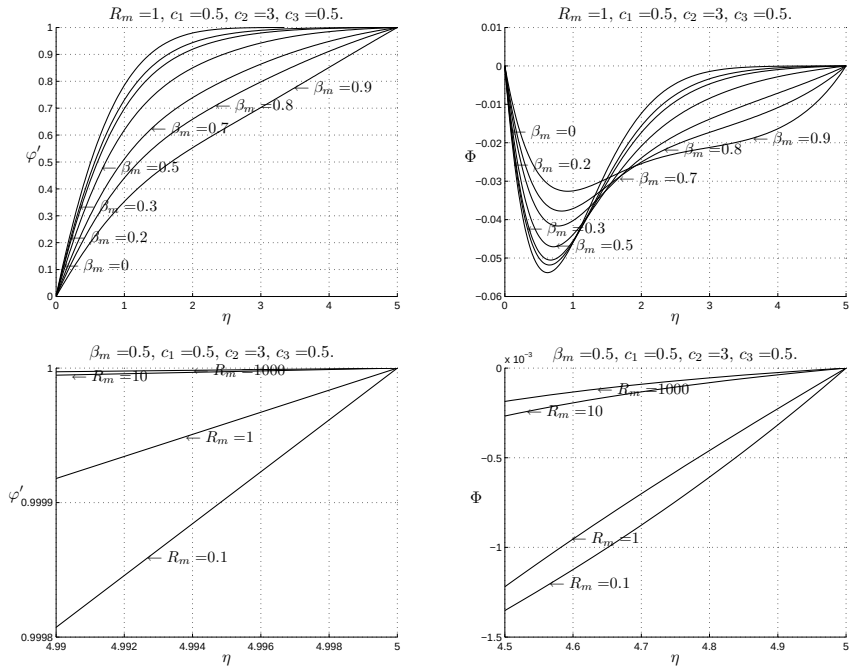

Figure 9: Plots showing φ' and Φ for different β_m and R_m, respectively.

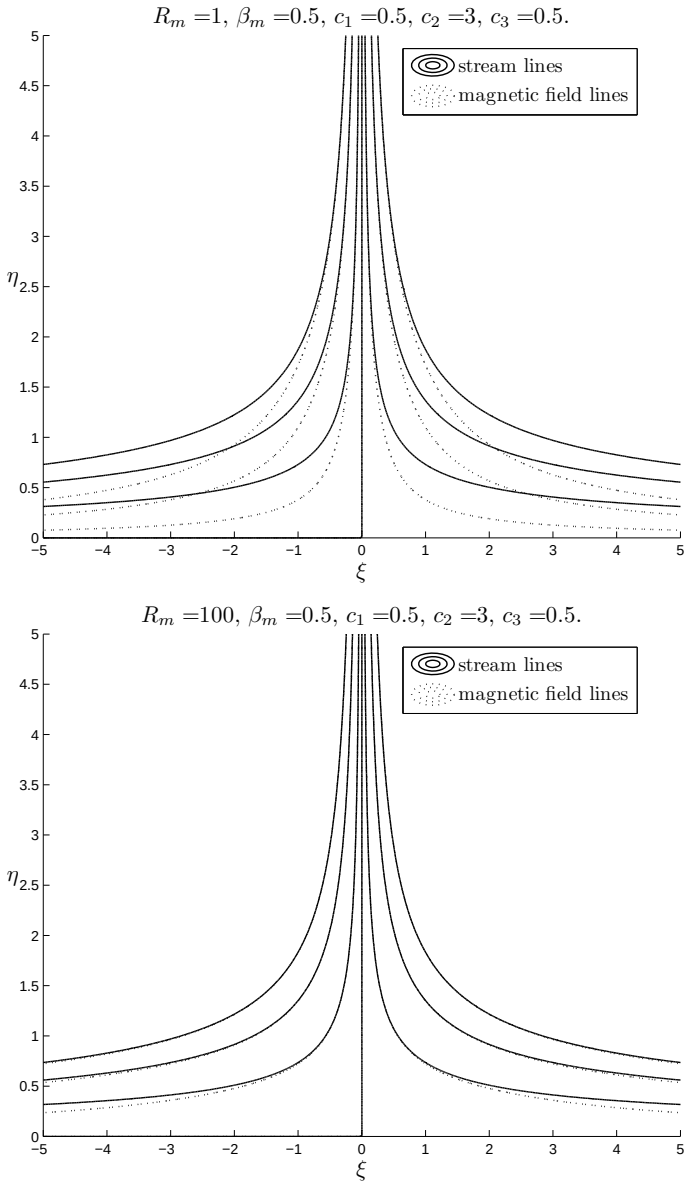

Figure 10: Figures show the streamlines for $c_1 = 0.5$, $c_2 = 3.0$, $c_3 = 0.5$, $\beta_m = 0.5$ and $R_m = 1$ or $R_m = 100$, respectively.